Influence of source on 2-D site effects

Petros Triantafyllidis and Panagiotis M. Hatzidimitriou
Geophysical Laboratory Aristotle University, Thessaloniki, Greece

Peter Suhadolc
Department of Earth Sciences, University of Trieste, Trieste, Italy

Received 2 August 2001; revised 12 February 2002; accepted 19 February 2002; published 26 March 2002.

[1] The site response has been theoretically estimated along seven 2-D profiles distributed in the broader urban area of Thessaloniki. The hybrid method employed allows the simulation of various events located at different distances and azimuths around the city. We focus on the results obtained at all points where the profiles intersect. The diversity of the ''site response'' at each intersection is attributed mainly to the influence of the seismic source, suggesting that the ground response does not depend only on local soil characteristics but also on different earthquake ''scenarios'' generating the impingent wavefield. *INDEX TERMS:* 7212 Seismology: Earthquake ground motions and engineering

1. Introduction

[2] Significant research work during the past two decades concerns the problem of ground response estimation (e.g. [*Kawase and Aki*, 1990; *Field and Jacob*, 1995]). Most of this research has been carried out à posteriori (i.e. after the occurrence of a destructive earthquake) using mainly experimental methods such as Standard Spectral Ratio (SSR), Horizontal to Vertical Spectral Ratio (HVSR), etc. Recently, several theoretical methods (such as finite differences, finite elements or modal summation) have been employed in order to develop 1-D, 2-D or 3-D numerical techniques for an à priori estimation of ground amplification (e.g. [*Panza and Suhadolc*, 1987; *Furumura and Takenaka*, 1996; *Field et al.*, 2000]). The question that arises is whether the response estimated at a specific site depends only on the local geological and geotechnical characteristics or on other factors as well. In this paper, we study the uniqueness of the so-called site effect by examining the source influence on the ground amplification variations. We conclude that different earthquake source scenarios generating the wavefield impingent on the site lead to a mean variation of factor of two in the amplification of the site.

2. Data and Method Used

[3] The present study concentrates in the city of Thessaloniki (N. Greece) for which we have used all the available data from borehole measurements (e.g. [*Raptakis et al.*, 1994; *Pitilakis and Anastasiadis*, 1998]) to construct seven 2-D profiles with different orientation, as is shown in Figure 1. The geometry and the other soil properties such as densities, body wave velocities and quality factors (Table 1), allow the definition of the 2-D ''local'' velocity models along each section. Each local model is underlain by the regional velocity model, as this is derived for the broader area of the Serbomacedonian zone [*Ligdas and Lees*, 1993; *Papazachos*, 1998], which we assume that consists of homogeneous and horizontal layers. Several double-couple point sources located at different epicentral distances and azimuths from the city were used to produce the synthetic acceleration wavefield for all components of motion. The fault plane solutions characterizing these sources, correspond either to known focal mechanisms of large destructive events (e.g. Thessaloniki 1978) or to mechanisms which are representative of the active stress field in the area of northern Greece [*Papazachos and Kiratzi*, 1996]. Table 2 shows the parameters of these sources, such as epicentral distance, magnitude, depth and fault plane solution used. The event which is the wavefield generating source for section CC, refers to the main

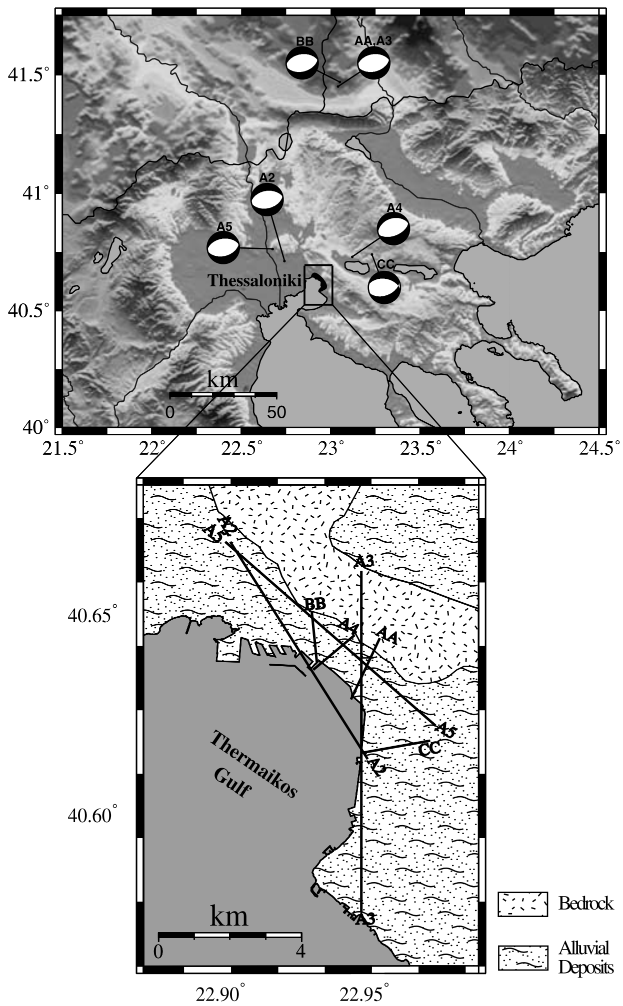

Figure 1. Map of the region, showing the location and the focal mechanisms of the events used for the simulations (up). The box which bounds the urban area around Thessaloniki, is enlarged below giving in details the length and the orientation of the cross sections along which the seismic response was estimated with the hybrid method.

0094-8276/02/2001GL013870$05.00

Table 1. Average Values of the Soil Properties Used in the 2-D Computations

Formation	Density (g/cm^3)	V_P (m/sec)	V_S (m/sec)	Q_P	Q_S
F1	1.85	450	225	60	20
F2	1.9	1750	225	60	20
F3	2.0	1600	280	100	40
F4	1.9	1700	280	50	15
F5	2.0	1700	350	60	20
F6	1.9	1800	370	50	15
F7	1.7	1600	180	70	25
F8	2.0	1900	450	50	15
F9	2.0	1600	500	70	25
F10	2.0	2000	700	60	20
F11	2.1	2500	650	100	50
F12	2.2	2800	750	120	60
F13	2.2	3200	850	150	80
Rock	2.5–2.6	4500	1500–1900	250	200

The geometry of each formation is outlined in Figure 2.

Table 2. Main Features of the Events Used for the Simulations

Section	R[a]	M_w	D[b]	Strike	Dip	Rake
AA	90.6	3.3	7	76°	45°	−94°
BB	91.4	4.7	7	76°	45°	−94°
CC	26.5	6.5	6	278°	46°	−70°
A2	15.5	2.5	6	76°	45°	−94°
A3	89.7	3.3	7	76°	45°	−94°
A4	17.2	5.1	6	252°	37°	−88°
A5	23.7	2.0	5	76°	45°	−94°

[a] Epicentral Distance (km).
[b] Depth (km).

earthquake of 1978 that struck the city causing considerable damage, while the event related to section A4 refers to its largest aftershock.

[4] The hybrid method employed for the computation of the ground response along the various profiles is described in detail elsewhere [*Fäh*, 1992; *Fäh and Suhadolc*, 1994; *Fäh et al.*, 1994] and combines the modal summation and the finite difference methods. The former one allows us to generate the wavefield and to take into account the path from the source position to the boundary of the target area, while the latter permits the modeling of wave propagation in complicated and rapidly varying velocity structures within the target area, as is required when dealing with sedimentary basins, like that in Thessaloniki.

3. Spectral Ratios

[5] Two sets of synthetics have been obtained, by a) assuming the receivers are underlain by the regional 1-D velocity model and b), by placing the receivers on top of the 2-D laterally heterogeneous velocity model characteristic of each considered profile (Figure 2). The simulations have been performed for all components of motion and for all frequencies up to a maximum cutoff frequency of 6 Hz. For each virtual receiver along the section, the spectrum of the synthetic accelerogram calculated from the local 2-D model was divided by the respective synthetic spectrum for the same receiver from the accelerograms computed using the 1-D regional model.

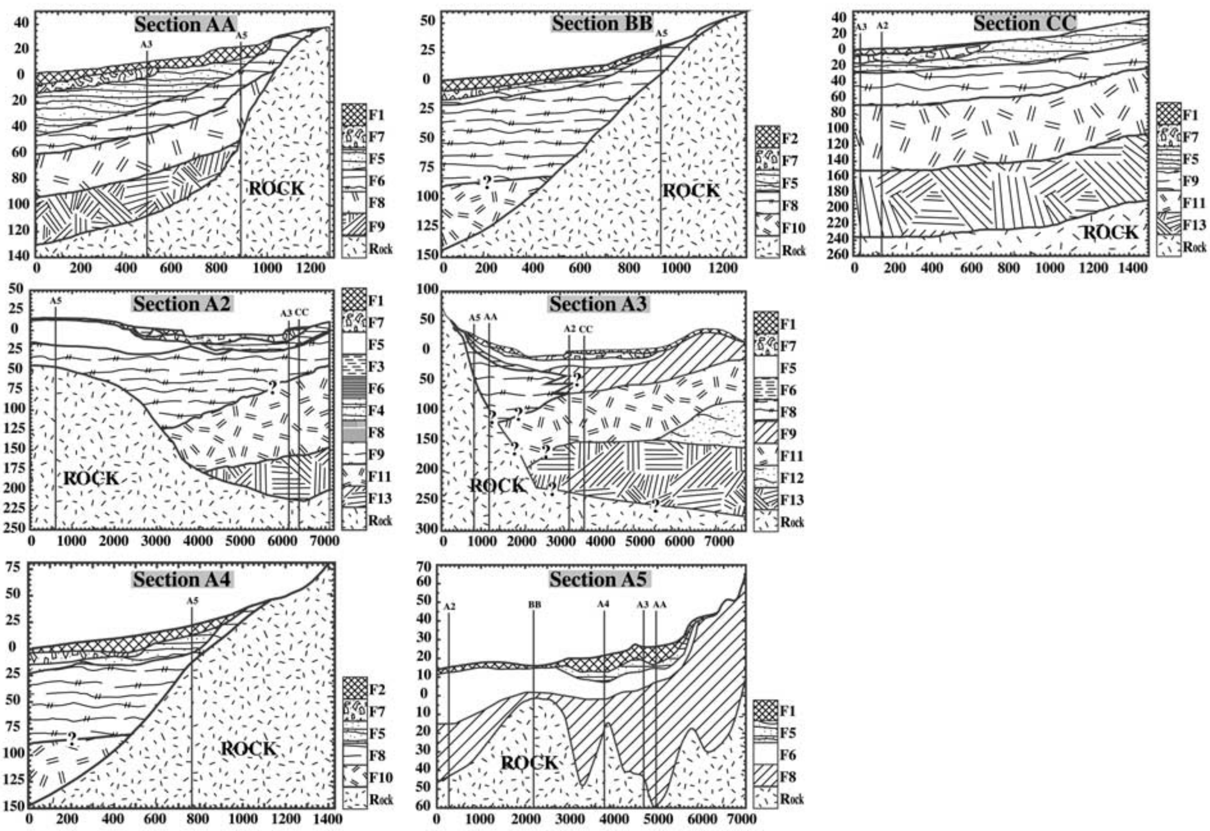

Figure 2. The seven 2-D geological profiles along which the seismic response was estimated with hybrid method. The question marks on sections BB, A2, A3, and A4 denote the poor knowledge of formation boundaries. The vertical lines indicate the intersection points between the considered profiles. Axes units are in meters.

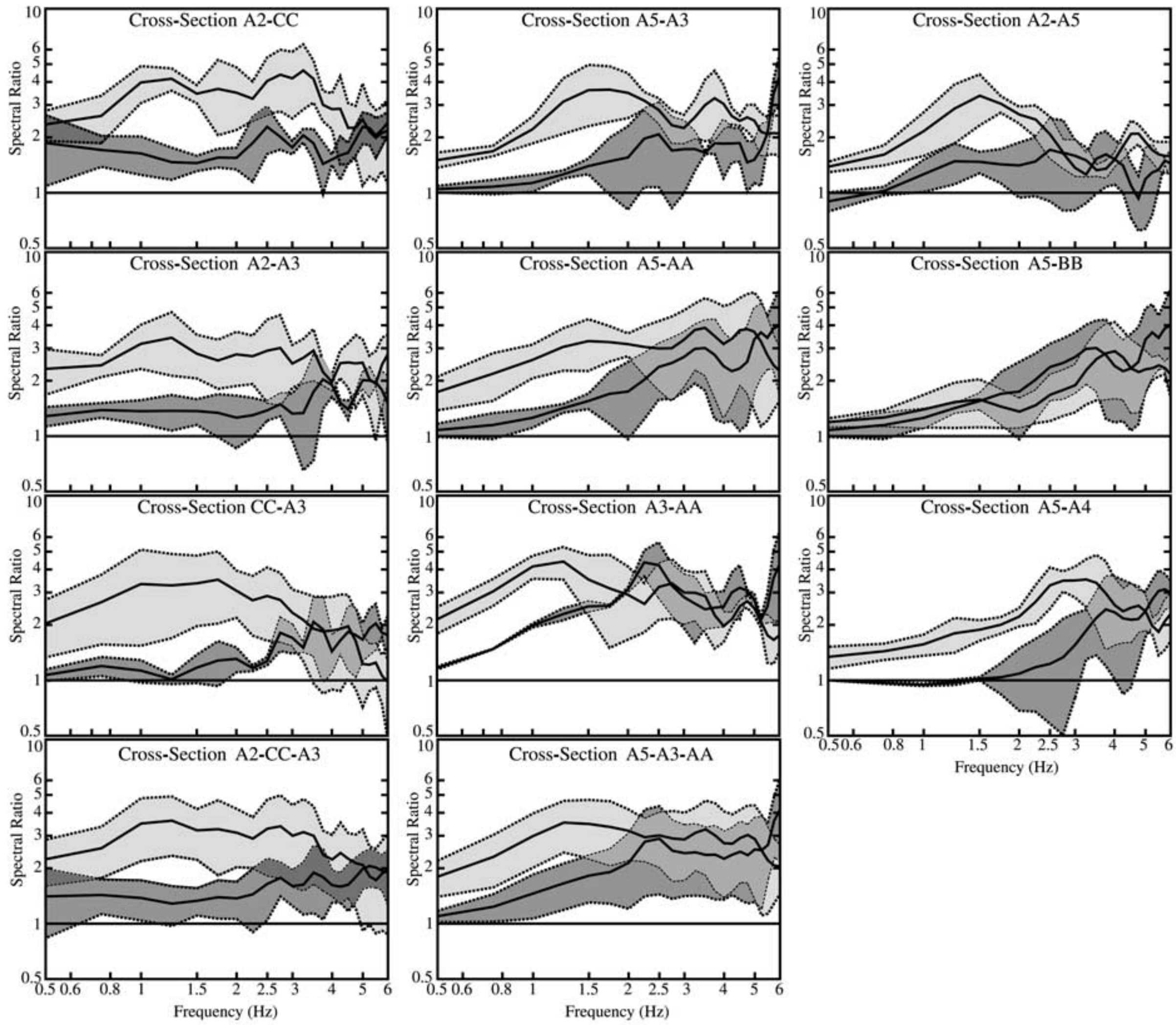

Figure 3. Means of spectral amplification between the ratios calculated at the common points of cross sections (solid lines). Shaded areas show the variation range plus/minus one standard deviation of the average of horizontal (light area) and vertical mean ratio (dark area).

[6] In this paper we focus on the comparison of the ground response in terms of such spectral ratios at the intersection points between various sections. Since the local geological model under an intersection point is common to both profiles, the differences in the obtained results can only be due to the different excitation of the incoming wavefield and the differences of propagation along the 2-D profiles. The purpose of this comparison is, therefore, to check in the most reliable way the response of each intersection point to different earthquake ‘‘scenarios’’, i.e. earthquakes generated at variable distances, directions as well as with variable focal mechanisms and magnitudes.

4. Results

[7] Examining the cross sections along which the ground response was estimated through the hybrid method (Figure 1, Table 2), the nine intersection points can be classified into three categories according to their mean distance from the corresponding seismic sources. One category consists of intersection points such as A3-AA, where the events used to generate the input wavefield are located at a distance of about 90 km from the first virtual receiver. The second category, consists of points that belong to sections which are both close to their wavefield generating sources, i.e. from 15.5 to 26.5 km approximately. To this category belong the intersection points of profiles A2-CC, A2-A5 and A5-A4. Finally, the third group consists of intersection points for which one of the corresponding sections is far from the wavefield generating source (around 90 km), while the other one is located in distances less than 30 km. These are the intersection points of profiles A5-BB, A5-A3, A5-AA, A2-A3 and CC-A3.

[8] In Figure 3, the solid lines represent the mean ground amplification (using the spectral ratios calculated with hybrid method along the two or three intersecting profiles), at the intersection points of these profiles. Shaded areas show the variation zone of the mean spectral ratios plus/minus one standard deviation. Light shaded bands are the areas where the average of the horizontal components (radial and transverse) variates (thick line), while the dark shaded area is the corresponding zone for the vertical mean ratio (thin line).

[9] On the first column of graphs in Figure 3 the deviation of mean ratios at points A2-CC (first row), A2-A3 (second row) and CC-A3 (third row) is presented. Although these points are very close to each other, we observe differences both in the spectral shape as well as in the amplification level and in the frequency

where the maximum amplification occurs. These differences are obvious for both components, horizontal and vertical. Since the regional 1-D velocity model underneath the whole area is the same, the effects of the propagation path up to the target area are thus minimized. Moreover, the site profile is almost identical for the three points and hence, the main factor giving rise to these differences is the variability of the seismic wavefield generating sources (mechanism and distance) used for those simulations (Table 2, Figure 1).

[10] In the last graph of the same column, the mean ratios present the total average ground response of the whole area limited by the previous points. It is clear that both horizontal and vertical means are somehow smoothed with no sharp peaks or troughs and with their standard deviation being almost constant for all the considered frequency range.

[11] An analogous situation is noticed in the second column of Figure 3, which presents the variation of the means at points A5-A3 (first row), A5-AA (second row) and A3-AA (third row). The smoothing of the average ground response in the last graph is even more obvious and the standard deviation zone is even wider, especially for the vertical component, particularly at low frequencies (below 2.5 Hz). The last column of graphs of Figure 3 consists of points which are far from each other (i.e. different soil profiles for each of them) and their results can only be presented independently.

5. Discussion and Conclusions

[12] The obtained results show that the source plays an important role in the site response, which varies according mainly to the source location (i.e. epicentral distance and azimuth). These different source characteristics produce variances of the expected mean site response, which are reflected in the standard deviation of that mean. The expected mean site response and its standard deviation are more reliable, as more points (i.e. sources) are taken into account in the calculation of the mean. This procedure is essential when microzonation is applied to a large urban area, since high vulnerabilities require extra caution in the computations of the expected ground response. Therefore, the site effect estimated at one location and based only on one simulated earthquake is not adequate to fully describe the response of the investigated site that could be taken as representative of the response of all future events to occur anywhere around the area of interest. The same might also be argued for the ground response estimated using experimental techniques. The lack of suitable data has prevented the realization of such studies. In conclusion, for a detailed microzonation study, the ground response at a given location must be examined for various earthquake scenarios, i.e. earthquakes with different focal mechanisms, epicentral distances, azimuths and magnitudes, compatible with the characteristics of the active faults in the surrounding areas. In this way, the expected site amplification estimated theoretically should be expected to be much more reliable.

[13] **Acknowledgments.** We are grateful to K. Pitilakis for providing borehole data, as well as to A. Anastasiadis for his help in constructing the simplified cross sections. We would like to thank also N. Theodulidis and G. F. Panza for fruitful discussions and C. B. Papazachos and A. Kiratzi for reading the final manuscript. This work was financially supported by EC project EVG1-CT-2001-00040.

References

Fäh, D., A hybrid technique for the estimation of strong ground motion in sedimentary basins, Ph.D. thesis, Nr 9767, 161 pp., Swiss Federal Institute of Technology, Zurich, 1992.

Fäh, D., and P. Suhadolc, Application of numerical wave-propagation techniques to study local soil effects: The case of Benevento (Italy), *Pure Appl. Geophys.*, *143*, 513–536, 1994.

Fäh, D., P. Suhadolc, St. Müller, and G. F. Panza, A hybrid method for the estimation of ground motion in sedimentary basin: Quantitative modeling for Mexico City, *Bull. Seismol. Soc. Am.*, *84*, 383–399, 1994.

Field, E. H., and K. Jacob, A comparison and test of various site response estimation techniques, including three that are non reference-site dependent, *Bull. Seismol. Soc. Am.*, *82-6*, 2283–2307, 1995.

Field, E. H., Accounting for site effects in probabilistic seismic hazard analyses of Southern California: Overview of the SCEC Phase III Report, *Bull. Seismol. Soc. Am.*, *90*(6B), S1–S31, 2000.

Furumura, T., and H. Takenaka, 2.5-D modeling of elastic waves using the pseudospectral method, *Geophys. Res. Lett.*, *25*, 785–788, 1996.

Kawase, H., and K. Aki, Topography effect at the critical SV waves incidence: Possible explanation of damage pattern by the Whittier Narrows, California, earthquake of 1st October 1987, *Bull. Seismol. Soc. Am.*, *80*, 1–22, 1990.

Ligdas, C. N., and J. M. Lees, Seismic velocity constraints in the Thessaloniki and Chalkidiki areas (Northern Greece) from a 3-D tomographic study, *Tectonophysics*, *228*(9), 7–121, 1993.

Panza, G. F., and P. Suhadolc, Complete strong motion synthetics, in *Seismic Strong Motion Synthetics, Computational Techniques 4*, edited by B. A. Bolt, pp. 153–204, Orlando, Academic Press, 1987.

Papazachos, C. B., Crustal P- and S-velocity structure of the Serbomacedonian Massif (Northern Greece) obtained by non-linear inversion of travel times, *Geophys. J. Int.*, *134*, 25–39, 1998.

Papazachos, C. B., and A. A. Kiratzi, A detailed study of the active crustal deformation in the Aegean and surrounding area, *Tectonophysics*, *253*, 129–153, 1996.

Pitilakis, K. and A. Anastasiadis, Soil and site characterization for seismic response analysis, *Proc. 11th ECEE, Paris 6–11 September, France*, 65–90, 1998.

Raptakis, D., E. Karaolani, K. Pitilakis, and N. Theodulidis, Horizontal to vertical spectral ratio and geological conditions: The case of a downhole array in Thessaloniki (Greece), *Proc. XXIV Gen. Ass. ESC, Athens, Greece*, *3*, 1570–1578, 1994.

P. Triantafyllidis and P. M. Hatzidimitriou, Geophysical Laboratory, Aristotle University of Thessaloniki, P.O. Box 111, Thessaloniki, 54124 Greece. (trian@lemnos.geo.auth.gr; takis@lemnos.geo.auth.gr)

P. Suhadolc, Department of Earth Sciences, University of Trieste, V. Weiss 1, 34127 Trieste, Italy. (suhadolc@dst.univ.trieste.it)